Protein Phase Behavior in Aqueous Solutions: Crystallization, Liquid-Liquid Phase Separation, Gels, and Aggregates

André C. Dumetz, Aaron M. Chockla, Eric W. Kaler, and Abraham M. Lenhoff
Center for Molecular and Engineering Thermodynamics, Department of Chemical Engineering, University of Delaware, Newark, Delaware 19716

ABSTRACT The aggregates and gels commonly observed during protein crystallization have generally been considered disordered phases without further characterization. Here their physical nature is addressed by investigating protein salting-out in ammonium sulfate and sodium chloride for six proteins (ovalbumin, ribonuclease A, soybean trypsin inhibitor, lysozyme, and β-lactoglobulin A and B) at 4°C, 23°C, and 37°C. When interpreted within the framework of a theoretical phase diagram obtained for colloidal particles displaying short-range attractive interactions, the results show that the formation of aggregates can be interpreted theoretically in terms of a gas-liquid phase separation for aggregates that are amorphous or gel-like. A notable additional feature is the existence of a second aggregation line observed for both ovalbumin and ribonuclease A in ammonium sulfate, interpreted theoretically as the spinodal. Further investigation of ovalbumin and lysozyme reveals that the formation of aggregates can be interpreted, in light of theoretical results from mode-coupling theory, as a kinetically trapped state or a gel phase that occurs through the intermediate of a gas-liquid phase separation. Despite the limitations of simple theoretical models of short-range attractive interactions, such as their inability to reproduce the effect of temperature, they provide a framework useful to describe the main features of protein phase behavior.

INTRODUCTION

The solubility of proteins has been the subject of measurements for more than a century, and the concept played a prominent role in the development of protein physical chemistry (1,2). Early investigations led to a few systematic measurements of protein solubility, particularly as a function of variables such as salt concentration, pH, or temperature (2,3). Some classic examples are still regularly cited, such as the work of Green on hemoglobin (4,5) or of Hofmeister on ovalbumin (6,7). However, the reliability of those studies is sometimes impaired by the limited purity of the proteins then used, as suggested by the often reported dependence of the protein crystal solubility on the initial protein concentration (8,9).

The solubility of precipitates, which can correspond to aggregates, gels, or liquid-liquid phase separation, has sometimes been measured (10–12), but it is only recently that the idea that their formation might correspond to a well-defined phase transition has emerged. Note that the phase behavior reported here concerns native proteins that do not undergo any significant conformational changes. Nonnative aggregation that can lead to gels, amorphous aggregates, or amyloid fibrils (13–15) is a fundamentally different physical phenomenon beyond the scope of this work.

The formation of native precipitates is typically interpreted as a positive sign in the search for conditions yielding crystals, and it is often used to optimize the concentration of a precipitant (16,17). The physical origin of such aggregates was first explored 3 decades ago when the existence of metastable liquid-liquid phase separations was demonstrated for different γ-crystallins (18–21) and lysozyme (21–25). Further investigation demonstrated that in the proximity of such liquid-liquid phase separations, those proteins behave as expected in terms of the theory of critical phenomena (26,27). Liquid-liquid phase separations of proteins could therefore be concluded to follow the same physics as other types of phase transitions (28).

The phase behavior of γ-crystallins, lysozyme (25,29–36), and more recently bovine pancreatic trypsin inhibitor (BPTI) (37,38) has been investigated. However, these studies generally dealt specifically with liquid-liquid phase separations, and the formation of gels has been reported in only a few cases for lysozyme in sodium chloride (25,39,40). In a recent investigation of the kinetics of lysozyme precipitation in ammonium sulfate, it was also suggested that the formation of aggregates corresponds to a frustrated liquid-liquid phase separation (41), but there has not been any extensive experimental investigation of the physical origin of aggregates, gels, and liquid-liquid phase separations. The main objective of this work is to compare experimental phase behavior observed for different proteins in light of recent theoretical developments in colloid phase behavior.

The potential of mean force (PMF) between protein molecules (42) is the central element in calculating protein phase diagrams. Because the PMF is a complex function of all the forces acting on protein molecules, its expression has to be approximated, and theoretical investigations of colloid phase behavior that aim to describe protein solutions are based on extremely simple expressions. PMF models

Submitted June 25, 2007, and accepted for publication August 9, 2007.

Address reprint requests to Abraham M. Lenhoff, Dept. of Chemical Engineering, University of Delaware, Newark, DE 19716. Tel.: 302-831-8989; Fax: 302-831-4466; E-mail: lenhoff@udel.edu.

Editor: Kathleen B. Hall.

0006-3495/08/01/570/14 $2.00

doi: 10.1529/biophysj.107.116152

typically neglect most of the complexity of protein interactions but still capture the general shape of the interaction potential. The PMF also governs the values of the second osmotic virial coefficient, b_2, which can be measured independently, and in this work data from the literature are used to show the effects of the additives investigated for some of the proteins considered.

Several different potentials have been used to qualitatively explain both protein phase behavior and the notion of the crystallization slot (43,44), which correlates b_2 with solution conditions favorable to protein crystallization (45–51). The phase diagrams predicted by these models, in the limit of very short-range attraction, are quite similar qualitatively, and the phase diagram calculated by Foffi et al. (52) (Fig. 1) for a short-range attractive Yukawa potential

$$\frac{U(r)}{k_BT} = \begin{cases} \infty & 0 \le r \le \sigma \\ -\frac{\epsilon}{k_BT}\frac{\sigma}{r}\exp[b(r-\sigma)] & \sigma < r \end{cases}$$

is used here as a reference to interpret the experimental phase behavior of proteins. In this expression, in which $U(r)$ is independent of temperature, r is the protein center-to-center separation distance, ε is the well depth of the Yukawa potential, σ is the protein hardcore diameter, and b^{-1} is a measure of the range of the Yukawa potential. In Fig. 1, which was obtained for $b\sigma = 7.5$, the dimensionless temperature $T^* = k_BT/\varepsilon$ is plotted for the different phase boundaries as a function of the protein volume fraction, Φ. This picture of the phase diagram should be well suited to describe protein phase behavior during protein salting-out when electrostatic interactions are screened (53,54). However, small changes in the PMF can have large effects on the phase diagram (55).

By definition, decreasing T^* is equivalent to decreasing temperature or increasing the attraction between proteins, and

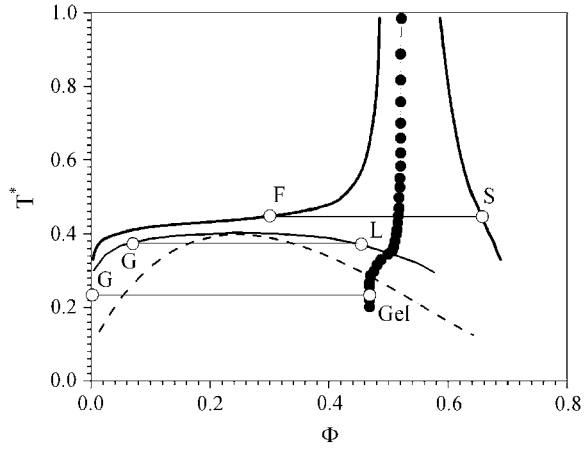

FIGURE 1 Theoretical phase diagram ($T^* = k_BT/\varepsilon$ versus volume fraction) calculated for the Yukawa potential ($b\sigma = 7.5$) by Foffi et al. (52) (see text). The solid lines correspond to the F, S and G, L phase separations, the dashed line represents the spinodal, and the solid circles correspond to the gelation line calculated from mode-coupling theory.

both interpretations are useful in interpreting the experimental phase behavior of proteins. However, because most of the results in this work are obtained at constant temperature as a function of increasing salt concentration, decreasing T^* will, at least initially, be interpreted as increasingly attractive interactions.

Different regions can be distinguished in the phase diagram in Fig. 1. The fluid-solid equilibrium (F, S) corresponds to protein crystals in equilibrium with their supernatant, so the solid line F represents the solubility. However, for most proteins nucleation does not occur readily, so the metastable region below the solubility and solid lines is almost always accessible. The gas-liquid phase separation (G, L) occurs if T^* continues to decrease below the solubility line, although it corresponds to a thermodynamically metastable state. Experimentally, this transition is manifested as a liquid-liquid phase separation between a liquid dilute in protein (the theoretical gas) and a dense liquid rich in protein (the theoretical liquid). The metastability of the gas-liquid phase separation is found theoretically for the Yukawa potential when the range of the interactions is $<\sim 1/6$ of the hard-core diameter (52,56). As a consequence, the metastability of the liquid-liquid phase separation observed for γ-crystallins, lysozyme, and BPTI has been viewed as a direct consequence of the short-range nature of protein interactions.

Two main regions can be distinguished below the gas-liquid binodal. Between the binodal (G, L) and the spinodal (*dashed line*), the gas-liquid phase separation occurs by nucleation of small drops of the dense liquid phase, which grow until the solution reaches equilibrium, whereas below the spinodal, the phase separation occurs instantaneously through spinodal decomposition. As a consequence, the kinetics of the gas-liquid phase separation differs depending on the mechanism by which the phase separation occurs.

In addition to these equilibria, the nonequilibrium states displayed by colloidal systems have recently been the subject of renewed interest, stimulated by theoretical results from mode coupling theory (MCT) (52,57–61). Several articles present a clear picture of the theoretical phase diagram and the expected routes to gel formation relevant to protein solutions (52,62). The gelation line calculated from MCT divides the theoretical phase diagram into two regions (Fig. 1). The region on the right side corresponds to a dynamically arrested state in which the solution forms a gel or glassy phase. Moreover, because the gelation line intersects the binodal, when a gas-liquid phase separation occurs, two situations are possible. For T^* values above the intersection of the gelation line with the binodal, gas-liquid phase separation occurs as described previously. Below the intersection of the binodal with the gelation line, the liquid phase cannot form, and the gas-liquid phase separation leads instead to the formation of a gel that can be viewed as a frustrated liquid. According to this scenario, the protein concentration in the dense gel phase should correspond to that at the intersection of the gas-liquid tie line with the gelation line.

Experimental data are presented here for six proteins covering a large range of molecular mass and pI values. The proteins are ovalbumin (pI 4.9, 45 kDa) (63), ribonuclease A (pI 9.6, 13.7 kDa) (64), soybean trypsin inhibitor (STI) (pI 4.5, 21.5 kDa) (65,66), β-lactoglobulin A (pI 5.23, 18.3 kDa) and B (pI 5.3, 18.3 kDa) (67,68), and lysozyme (pI 11, 14.3 kDa) (69), and their phase behavior is investigated in ammonium sulfate solutions at pH 7. The phase behavior of lysozyme was also determined in sodium chloride at pH 7 to compare the results here with previous reports.

Ammonium sulfate, which is among the best crystallization agents (16,70), was chosen because of its strong salting-out properties; among the proteins studied, lysozyme is the only one to precipitate in sodium chloride. β-Lactoglobulin A and B, which differ only by two amino acids (Asp/Gly-64 and Val/Ala-118) (68), and STI have also been reported to salt-in in the neighborhood of their isoelectric point (66,67,71,72), but the investigations here were restricted to pH 7, and consequently only protein salting-out is relevant.

The results are organized around four foci. First, the phase behavior for the six proteins is presented by documenting the appearance and kinetics of formation of the different phases. Second, the physical nature of the precipitates is investigated in more detail for ovalbumin and lysozyme. Third, the correlation between the positions of the aggregation and solubility lines and the second osmotic virial coefficient is discussed, and finally, failure of the theoretical phase diagram (Fig. 1) to capture the temperature dependence observed experimentally is emphasized to show the limit of current theoretical approaches.

MATERIALS AND METHODS

Proteins and chemicals

Ovalbumin was obtained from fresh single-comb white Leghorn eggs following the purification protocol used by Judge et al. (73,74). β-Lactoglobulin from bovine milk (L0130) and lysozyme from chicken egg white (L6876) were purchased from Sigma (St. Louis, MO), STI (21730) was obtained from USB (Cleveland, OH), and ribonuclease A (LS003433) was purchased from Worthington (Lakewood, NJ). Sodium chloride (S-271) and sodium phosphate (P-285) were obtained from Fisher Scientific (Hampton, NH). Ammonium sulfate (A-2939) was purchased from Sigma.

Protein purification

Lysozyme was the only protein found to be consistently free of impurities before purification. Others, even when specified as ultrapure by the manufacturer, had different degrees of impurities that could vary among lots. For this reason, all proteins were purified chromatographically using an ÄKTA Purifier from GE Healthcare (Piscataway, NJ). The only exceptions were the lysozyme solutions used to determine the protein concentration in the precipitate, which were only dialyzed.

Chromatography was performed at pH 7 using 5 mM sodium phosphate as the low-salt buffer and 2 M sodium chloride, 5 mM sodium phosphate as the high-salt buffer. Two resins, SP Sepharose FF and Q Sepharose FF (GE Healthcare) were used for cation and anion exchange of the basic and acidic proteins, respectively. Two types of columns, XK16 and XK 28 (GE Healthcare), were used. Once purified, the protein solutions were reconcentrated to 30–60 mg/mL using an Amicon stirred ultrafiltration cell (model 8200) equipped with a YM10 ultrafiltration membrane, both purchased from Millipore (Billerica, MA). The protein solutions were then dialyzed extensively against 5 mM sodium phosphate, pH 7, using a 10 mL Slide-A-Lyzer cassette from Pierce Biotechnology (Rockford, IL). The last step was to reconcentrate protein solutions up to 100–150 mg/mL using a 10k MWCO Amicon Ultra-4 centrifugal filter device from Millipore.

Concentrations were measured by ultraviolet (UV) absorbance at 280 nm using a Lambda 4B spectrophotometer from Perkin-Elmer (Foster City, CA). The extinction coefficients were taken as $E^{1\%}_{1cm} = 7.35$ for ovalbumin, 7.14 for ribonuclease A, 9.1 for STI, 26.0 for lysozyme, and 9.5 for β-lactoglobulin A and B (75). The purity of the final material was checked by gel electrophoresis.

Phase behavior experiments

The samples for phase behavior observations were prepared by pipetting appropriate amounts of three different stock solutions that were mixed together in the order high salt, low salt, and concentrated protein stock solutions. Sodium phosphate, the pK_a values of which are known to depend little on temperature, was used in all the experiments, with the same buffer concentration (5 or 100 mM sodium phosphate) in the three different stock solutions. A total volume of 200 μL was prepared in 0.5 mL tubes (05-408-120) from Fisher Scientific for each sample, and all of them were mixed immediately at the end of the preparation procedure.

For each sample, between 7 and 10 μL were pipetted into a 72-well microplate (HR3-087) and covered with paraffin oil (HR3-421), both from Hampton Research (Aliso Viejo, CA). The operation was repeated six times for each sample so that each column on the 72-well plate corresponded to the same solution condition. This was found to be an accurate way to ensure the consistency and reproducibility of the experimental observations and to follow their evolution over time.

The measurements as a function of temperature were performed by preparing three different microplates for each set of solution conditions. One was kept at room temperature for the measurements at 23°C, one was refrigerated for the measurements at 4°C, and the third was placed in an incubator for the measurements at 37°C.

The phase behavior was documented using a Leitz Laborlux S microscope equipped with a universal digital coupler (Mel Sobel Microscopes, Hicksville, NY) and a Nikon Coolpix 8700 digital camera (Nikon, Tokyo, Japan). All the microplates were observed just after preparation and then daily for the first week. The phase behavior was subsequently recorded regularly over a period of a few months.

The aggregation line was defined as the concentration at which the transition from clear to cloudy samples was seen, and the error bar for each point was taken as the concentration difference between neighboring samples. Because of the higher supersaturation necessary for nucleation of crystals, lysozyme crystal solubility in sodium chloride was obtained by measuring the UV absorbance at 280 nm of the supernatant of crystallized protein samples prepared in the 0.5 mL tubes as described above.

Protein concentration in the dense phase

The protein concentration in the precipitate was determined by UV absorbance at 280 nm after separating the aggregates by ultracentrifugation and then redissolving them in deionized water. Three samples of 1.4 mL each were prepared for each salt concentration, starting from the same stock solutions as in the phase behavior experiments (low salt, high salt, and concentrated protein solutions). For lysozyme and ovalbumin a thick precipitate formed upon preparation, so after 1–2 h the samples were centrifuged at 50,000 rpm, 23°C, for 30 min using an Optima L-100XP ultracentrifuge from Beckman-Coulter (Fullerton, CA). Polyallomer Konical centrifuge tubes (358117) with adapters (358152) were used to minimize

protein consumption. The volumes of the supernatant and the aggregate pellet were measured. The supernatant was removed and the pellet was dissolved in 1 mL deionized water. The concentration of the solution thus obtained was measured by UV absorbance at 280 nm, and the equivalent protein concentration in the dense precipitate phase could be calculated.

RESULTS AND DISCUSSION

Forms of phase behavior

Phase diagrams were determined by preparing samples at given salt concentrations with different protein concentrations. For each salt concentration, each protein aggregates above a well-defined protein concentration. Fig. 2 shows the aggregation lines for ovalbumin, ribonuclease A, STI, β-lactoglobulin A and B, and lysozyme in ammonium sulfate, as well as for lysozyme in sodium chloride. The aggregation lines all have the same characteristic curvature, but aggregation occurs at a different concentration for each protein. In ammonium sulfate, ovalbumin aggregates around 2–2.3 M salt, ribonuclease A around 1–1.5 M, STI around 1.25–1.75 M, β-lactoglobulin A and B around 2.5–3 M, and lysozyme around 1.5–2 M (Fig. 2). Lysozyme in sodium chloride aggregates over a much wider range of salt concentrations from 1 to 4 M.

The aggregates visually had the same white appearance for all six proteins. The only exceptions were ovalbumin samples prepared close to the aggregation line, for which translucent aggregates formed at the surface of the tubes. However, ovalbumin aggregates with concentrations far from the precipitation line had the same visual appearance as those of the other proteins. All aggregates settled in less than a day after sample preparation, and they redissolved completely in deionized water. Despite these common features, the aggregates differed considerably among the different proteins in terms of their microscopic appearance and the kinetics of their formation.

Fig. 3 illustrates ovalbumin phase behavior 20 min after preparation in 2.2 M ammonium sulfate with increasing protein concentration, corresponding to a vertical path on the phase diagram (Fig. 2) at the given salt concentration. The last well shown, at 49.9 mg/mL, as well as the samples prepared at higher protein concentrations, were cloudy immediately upon preparation. The instantaneous formation of aggregates occurs above a well-defined concentration, and a clear transition in the kinetics of aggregation exists between the eighth and ninth wells. The samples at slightly lower protein concentration also precipitated rapidly and, after 20 min, only the first four wells were still free of aggregates. Ultimately, after 1 day, only the first two wells remained clear, and the aggregation line is defined as the transition between the second and third wells; this is the basis for the error bars in Fig. 2 and similar plots that follow.

Fig. 4 shows the evolution of the fifth well in Fig. 3 over a period of 10 days. The first aggregates, which were present after 20 min, grew gradually and formed gel beads that reached a size of ~50 μm after a few days. Similar observations were made in the third and fourth wells in Fig. 3, albeit with a delay in the growth of the gel-like aggregates. The fifth, sixth, and seventh wells in Fig. 3 were clear just after preparation, but aggregates developed rapidly. At high magnification, those aggregates had the appearance of gel beads during the first few minutes after sample preparation. Nevertheless, the aggregates in those wells did not grow as

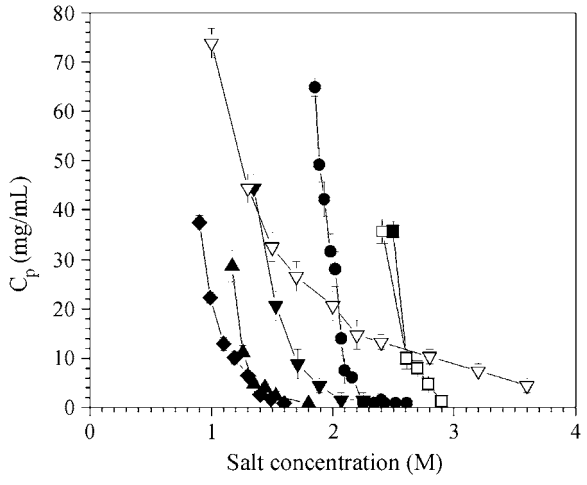

FIGURE 2 Aggregation lines for (♦) ribonuclease A, (▲) STI, (▼) lysozyme, (●) ovalbumin, (□) β-lactoglobulin B, and (■) β-lactoglobulin A in ammonium sulfate, and (∇) lysozyme in sodium chloride.

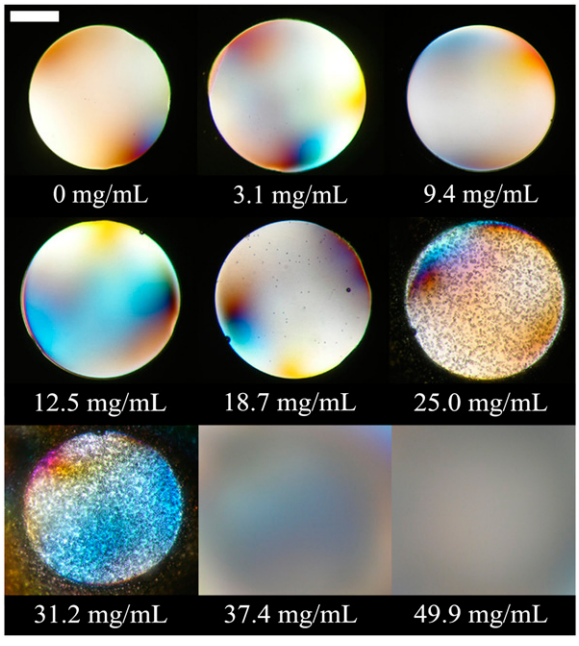

FIGURE 3 Phase behavior of ovalbumin after 20 min as a function of protein concentration in 2.2 M ammonium sulfate, 5 mM sodium phosphate, pH 7, 23°C. The scale bar represents 0.3 mm.

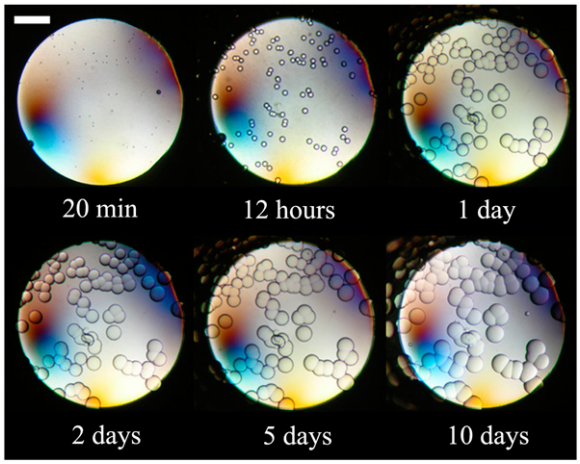

FIGURE 4 Evolution over time of ovalbumin at 18.7 mg/mL, 2.2 M ammonium sulfate, 5 mM sodium phosphate, pH 7, 23°C. The scale bar represents 0.3 mm.

large as did those at lower protein concentrations, and the microscopic gel beads that formed rapidly covered the entire surface of the well, so that the solution appeared cloudy. This is the reason for the appearance of the eighth well in Fig. 3 after 20 min, even though it was initially clear of aggregates.

Fig. 5 *A* shows the phase behavior after 2 weeks for a solution of ovalbumin prepared close to the aggregation line. The gel-like structure is apparent in that the beads did not coalesce as they would if they were liquid. Fig. 5 *B* shows the sharp edges formed by a bead that was broken mechanically, and this shape was unchanged for a month after the pictures were taken.

Ovalbumin crystallized sporadically in some of the wells at pH 7. Fig. 6 shows the kinetics of crystal growth for a solution in which needle-like crystals grew from a clear solution. However, this behavior was not sufficiently consistent to allow the position of the solubility line to be determined.

The phase behavior observed for ribonuclease A has some similarities with that of ovalbumin, but the microscopic appearance of the aggregates is clearly different. Fig. 7 shows a vertical cut of the phase diagram of ribonuclease A (Fig. 2) at

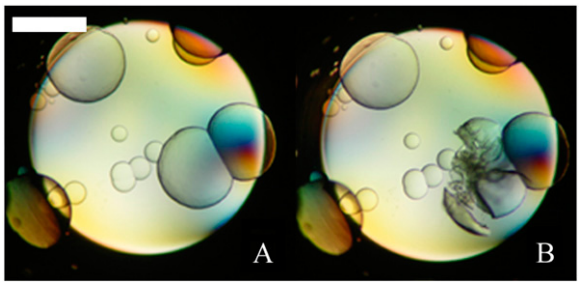

FIGURE 5 Ovalbumin gel beads obtained in ammonium sulfate after 2 weeks at pH 7, 23°C, close to the aggregation line (*A*) before and (*B*) after being broken. The scale bar represents 0.3 mm.

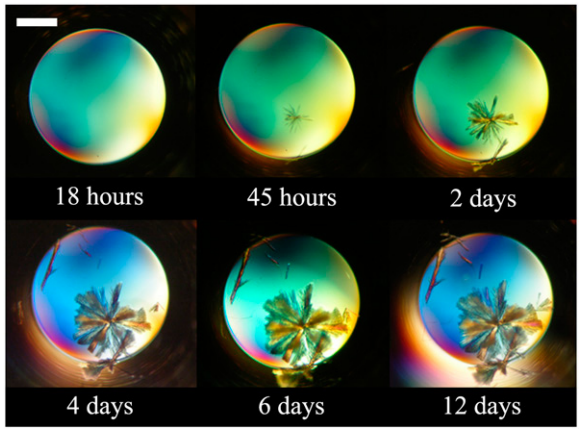

FIGURE 6 Evolution over time of ovalbumin at 5.8 mg/mL, 1.98 M ammonium sulfate, 5 mM sodium phosphate, pH 7, 23°C. The scale bar represents 0.3 mm.

1.6 M ammonium sulfate with increasing protein concentration 1 day after preparation. The last well and solutions prepared at higher protein concentrations were cloudy immediately upon preparation, as observed for ovalbumin. A clear transition in the kinetics of aggregation exists between the eighth and ninth wells. The sixth and seventh wells aggregated rapidly, and all the solutions at lower protein concentrations formed white-gray aggregates over a period of a few hours. The aggregates sedimented to the bottom of the wells within a day, and their appearance did not undergo any further changes after this initial period.

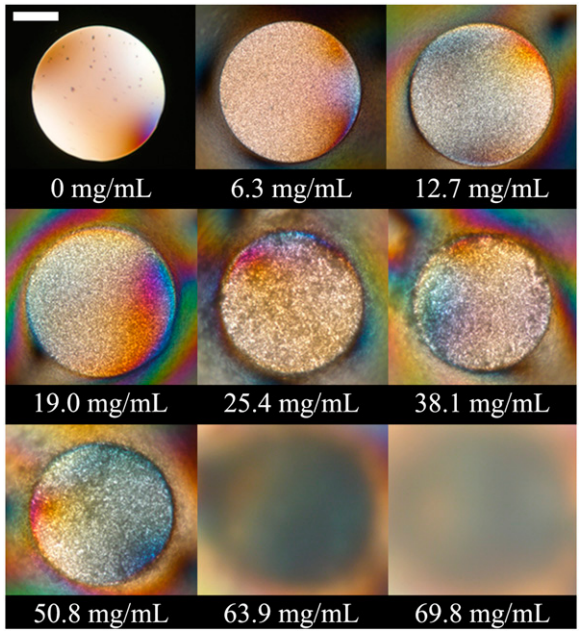

FIGURE 7 Phase behavior of ribonuclease A as a function of the protein concentration 1 day after preparation in 1.6 M ammonium sulfate, 100 mM sodium phosphate, pH 7, 23°C. The scale bar represents 0.3 mm.

Despite the differences in the microscopic appearances of ovalbumin and ribonuclease A aggregates, both proteins show a transition in the kinetics of aggregate formation at high protein concentrations. This transition, beyond which the solutions immediately became cloudy, was observed at a well-defined concentration. This concentration defines the second aggregation line that is shown for ovalbumin and ribonuclease A in Fig. 8 (the aggregation line shown in Fig. 2 will be referred to below as the first aggregation line). Between the first and second aggregation lines, ovalbumin and ribonuclease A aggregates correspond, respectively, to the formation of gel beads and fractal-like aggregates. Beyond the second aggregation line, the aggregates for both proteins had a white, shiny appearance that differed from the white-gray appearance in the first region. These previously unreported changes in ovalbumin and ribonuclease A phase behavior were made possible by this study's experimental protocol, which allows the entire surface of the phase diagram to be investigated systematically, and the evolution of the samples to be recorded over time.

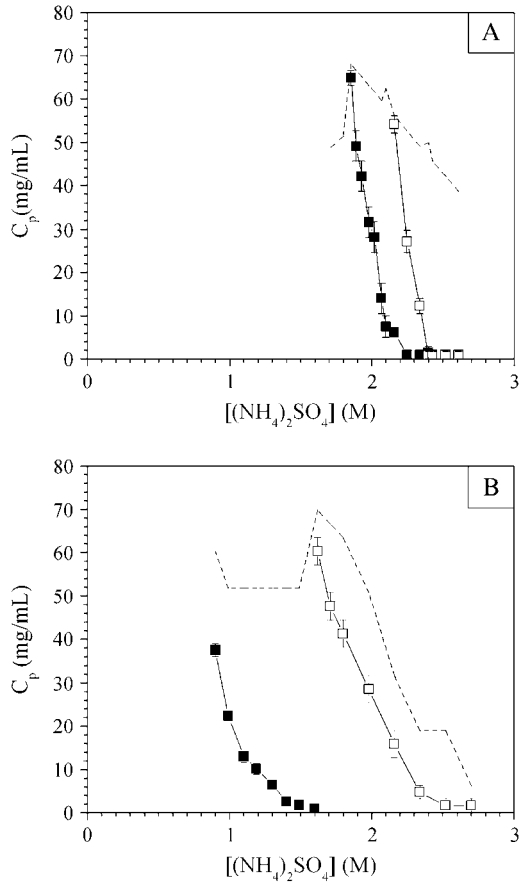

FIGURE 8 (■) First and (□) second aggregation lines for (*A*) ovalbumin and (*B*) ribonuclease A at 23°C. The pH was maintained at pH 7 by 5 mM sodium phosphate for ovalbumin and 100 mM sodium phosphate for ribonuclease A. The dotted line delimits the domain investigated experimentally.

The phase behavior obtained for STI, β-lactoglobulin A and B, and lysozyme was different in that only one aggregation line was observed experimentally. For STI the aggregates were similar in both their appearance and their formation kinetics to those obtained for ribonuclease A between the first and second aggregation lines. However, the phase behavior was investigated only over a restricted range of salt concentrations, and there may be an unobserved transition at higher salt concentrations.

For β-lactoglobulin A and B and lysozyme, aggregates formed almost instantaneously upon mixing even close to the first aggregation line, and no special characteristics were observed based on either the microscopic appearance or the kinetics of formation beyond the first aggregation line. The aggregates for these three proteins had a white, shiny appearance similar to that of ovalbumin and ribonuclease A aggregates beyond the second aggregation line.

Figs. 9 and 10 illustrate the kinetics of crystal formation for lysozyme in sodium chloride in the presence and absence of aggregates. Lysozyme crystallizes extremely easily in sodium chloride, and the results here are consistent with previous observations (11,25,32). Fig. 9 shows that in the absence of aggregates, crystals appeared in less than a day from a clear solution, and they reached a critical size after a couple of days. Fig. 10 shows that when aggregates formed first, they dissolved over a period of a few days and fed the growth of the crystals.

The main question that arises from the observations here concerns the physical origin of the different transitions. Fig. 1, which was explained in detail above, provides the theoretical framework needed to interpret the experimental results. Increasing the salt concentration in the range used here typically increases protein-protein attraction, presumably by hydration effects leading to salting-out (2,76). This would increase the depth of the potential ε and thus decrease T^* on the theoretical phase diagram.

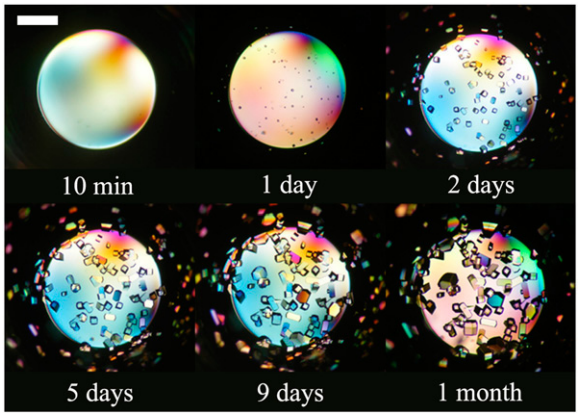

FIGURE 9 Evolution over time of lysozyme at 23.6 mg/mL, 1.3 M NaCl, 5 mM sodium phosphate, pH 7, 23°C. The scale bar represents 0.3 mm.

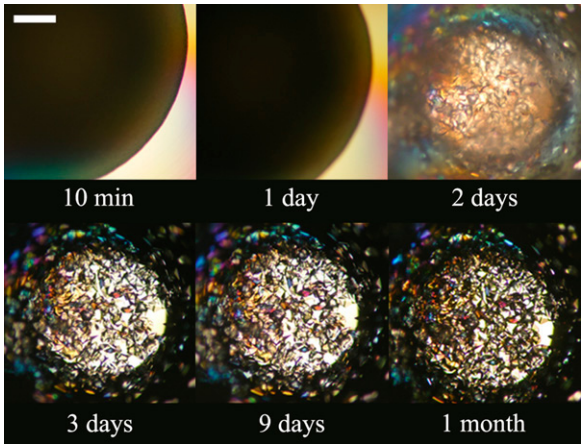

FIGURE 10 Evolution over time of lysozyme at 59.1 mg/mL, 1.3 M NaCl, 5 mM sodium phosphate, pH 7, 23°C. The scale bar represents 0.3 mm.

The protein concentrations typically explored experimentally (below ~150 mg/mL) correspond to small volume fractions, so it is chiefly the dilute Φ end of the phase diagram that is of interest. As the salt concentration is increased (decreasing T^*), a solution at a given protein concentration first crosses the fluid-solid phase boundary, which corresponds to the solubility line (Fig. 1). At a higher salt concentration, the solution reaches the gas-liquid phase boundary, where it should phase separate. The general shape of the first aggregation line (Fig. 2) is similar to the shape of the theoretical gas-liquid phase boundary, and the first aggregation line can consequently be identified as the gas-liquid phase separation, for which the liquid and the gas correspond to the aggregates and their supernatant, respectively. When the salt concentration is increased further, the solution finally reaches the spinodal, and the phase separation should be instantaneous. Following the previous analogy, the second aggregation line observed for ovalbumin and ribonuclease A can be interpreted as the spinodal line based on the difference in the kinetics of aggregation.

Despite the differences seen in the appearance of the aggregates among different proteins, the general shape of the theoretical phase diagram in Fig. 1 provides an overall picture of protein phase behavior that allows the different phase transitions to be identified. For ovalbumin and ribonuclease A, the two aggregation lines seem to reflect the difference in the aggregation kinetics when the gas-liquid phase separation occurs by nucleation or by spinodal decomposition. For β-lactoglobulin A and B and lysozyme, aggregates form rapidly beyond the first aggregation line, and the aggregation kinetics is such that the second aggregation line, if it exists, cannot be distinguished using the experimental procedures of this study.

The only spinodal decomposition measurements on proteins previously published were performed by light scattering as a function of temperature for lysozyme (22,27,77) and γ_{II}-crystallin (18), but the spinodal has been obtained for other (nonprotein) colloidal systems as a function of increasing precipitant concentration (78–82). The identification of the second aggregation line as the spinodal is consistent with those results.

For lysozyme, which crystallizes readily in sodium chloride at pH 7, the formation of crystals from a clear solution (Fig. 9) corresponds to the region between the fluid-solid and the gas-liquid phase boundaries on the theoretical phase diagram. The formation of crystals in the presence of aggregates (Fig. 10), on the other hand, corresponds to the region beyond the gas-liquid binodal. These results show that more than one route is available to crystallize proteins, and the presence of aggregates is not a barrier to protein crystallization. Conversely, aggregates can feed crystal growth.

However, crystallization depends on the existence of crystal contacts to allow the formation of a crystalline network and on nucleation to initiate this process. The intrinsic anisotropy of the crystal contacts makes use of the phase diagram based on an isotropic potential questionable, and this is compounded by the uncertainties inherent in representing nucleation on the phase diagram. Therefore, despite the importance of these issues, they were not addressed in this investigation.

Experimental gelation line for ovalbumin and lysozyme

The theoretical picture of protein phase behavior in Fig. 1 matches most of the experimental observations in that it reproduces the shape of the aggregation line and explains the existence of a second aggregation line. However, the appearance of the aggregates for ovalbumin suggests that the dense phase corresponds not to a liquid but to a gel. When ultracentrifuged, protein aggregates form a pellet instead of two clear phases separated by a sharp meniscus, which would be a signature of a liquid-liquid phase separation. Both those observations suggest that the observed protein aggregates do not correspond to a liquid-liquid phase separation as reported for lysozyme in sodium chloride (22,23,25).

As discussed in the Introduction, two situations are possible according to the theoretical phase diagram (Fig. 1). Above the intersection of the binodal with the gelation line, gas-liquid phase separation occurs, whereas below the intersection, the gas-liquid phase separation leads to the formation of a dynamically arrested phase corresponding to a gel. The protein concentration in the gel phase should correspond to that at the intersection of the gas-liquid phase separation tie line with the gelation line.

An experimental approach to test the physical nature of the dense aggregate phase, suggested by the relative slopes of the gas-liquid and gelation lines (Fig. 1), is to measure the protein concentration in the dense phase as a function of increasing salt concentration. If the protein concentration increases with salt concentration, this would be consistent with a gas-liquid phase separation, and the aggregates can be

identified as a liquid phase. A decrease in protein concentration in the dense phase with increasing salt concentration, on the other hand, would be consistent with the gas-liquid phase boundary intersecting the gelation line, and the aggregates can be identified as a gel phase.

The nature of the dense aggregate phase was investigated for ovalbumin in ammonium sulfate and lysozyme in ammonium sulfate and sodium chloride. For ovalbumin at pH 7 (Fig. 11 *A*) and for lysozyme in ammonium sulfate (Fig. 11 *B*), the protein concentration in the dense phase decreased with increasing ammonium sulfate concentration. However, for lysozyme in sodium chloride (Fig. 11 *C*) the protein concentration in the dense phase increases as the concentration of sodium chloride increased from 0.8 to 1.6 M, but it decreased above 1.6 M sodium chloride. The appearance of lysozyme aggregates upon preparation was the same below and above 1.6 M sodium chloride, but a change was observed in the appearance after centrifugation. Between 0.8 and 1.6 M sodium chloride, the lower phase was translucent, whereas above 1.6 M sodium chloride it had a white, shiny appearance similar to that before centrifugation.

These observations indicate that ovalbumin and lysozyme aggregates in ammonium sulfate result from a gas-liquid phase separation in which the dense phase does not reach the liquid state but instead is kinetically trapped as a gel phase. On the other hand, the results suggest that two regions should be distinguished when considering lysozyme aggregates in sodium chloride, namely a dense liquid between 0.8 and 1.6 M NaCl and a dynamically arrested gel phase above 1.6 M NaCl. Because the protein concentrations in the dense phases were determined after centrifugation, there is some uncertainty regarding how accurately the plotted dense phase concentrations represent the phases formed. Specifically, although the concentration in the liquid phase should not be affected by centrifugation, the apparent concentration in the gel may be changed due to a change in the microstructure, but despite this limitation, the global trend should remain the same.

Fig. 11 *D*, which contains the same basic information as Fig. 1, illustrates the relative positions of the theoretical phases. The right axis shows the protein concentration in mg/mL, based on lysozyme. The comparison between Fig. 11 *D* and the experimental results for ovalbumin and lysozyme allows the general shape of the phase diagram to be recognized and the different transitions to be identified.

As seen for ovalbumin and lysozyme aggregates in ammonium sulfate, the appearance of the aggregates can be different even if they have the same physical nature. Ovalbumin aggregates have a gel-like structure, whereas lysozyme aggregates have a white, shiny appearance, and both are described theoretically as a gel phase. This suggests that there is no difference, except in appearance, between gel bead aggregates that are often observed in crystallization screens and other types of native protein aggregates.

In contrast, some aggregates may have the same visual appearance and differ in their physical nature. For example, over the range of salt concentrations investigated, lysozyme in sodium chloride formed aggregates that had a white, shiny appearance after preparation, but Fig. 11 *C* reveals that the aggregates correspond to a liquid below ~1.6 M sodium

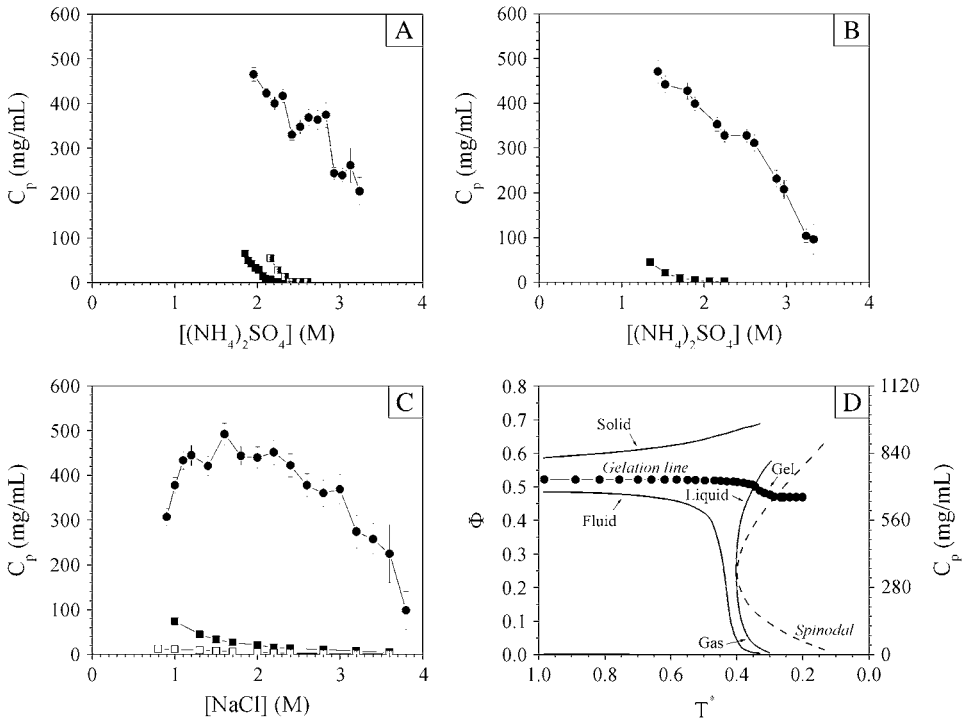

FIGURE 11 (◇) Crystal solubility, (■) first aggregation line, (●) aggregate solubility, and (□) second aggregation line in 5 mM sodium phosphate, pH 7, 23°C for (*A*) ovalbumin in ammonium sulfate, and for lysozyme in (*B*) ammonium sulfate and (*C*) sodium chloride. (*D*) Theoretical phase diagram (Fig. 1) oriented in the same direction as the experimental data.

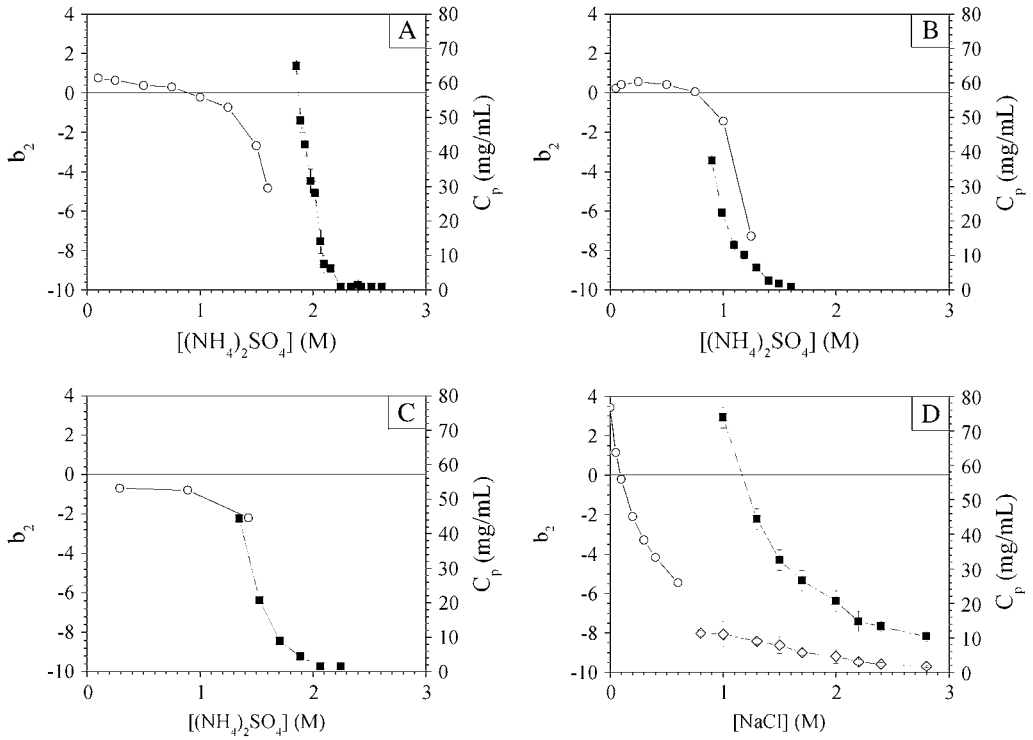

FIGURE 12 Comparison between (○) b_2 and (■) aggregation line at pH 7, 23°C for (*A*) ovalbumin in $(NH_4)_2SO_4$, (*B*) ribonuclease A in $(NH_4)_2SO_4$, (*C*) lysozyme in $(NH_4)_2SO_4$, and (*D*) lysozyme in NaCl. (◇) Solubility line for (*D*) lysozyme in NaCl. The b_2 values for ovalbumin and ribonuclease A in $(NH_4)_2SO_4$ (76) and lysozyme in NaCl (91) and $(NH_4)_2SO_4$ (90) were obtained from the literature.

chloride and to a gel phase above this concentration. Taratuta et al. (23), in their early experiments on lysozyme liquid-liquid phase separation in sodium chloride, obtained a sharp meniscus between two clear liquids only after ultracentrifugation (23). If the solution was not centrifuged, lysozyme crystallized before the phase separation occurred because of the high viscosity of the dense liquid phase.

The experimental investigations of lysozyme liquid-liquid phase separation previously published were performed at relatively low sodium chloride concentrations and high protein concentrations (22,23,25). There is consequently no discrepancy with the results of this work showing the existence of a gel phase at high salt concentrations. These results are also consistent with those of Sedgwick et al. (40), but the origin of the gel formation that was previously reported for lysozyme in sodium chloride by Muschol and Rosenberger and by Kulkarni et al. remains unclear (25,39). This might be due to lysozyme clustering at high protein concentrations (83,84).

Although the results show the existence of a liquid-liquid phase separation for lysozyme in sodium chloride, its existence for lysozyme and ovalbumin in ammonium sulfate remains hypothetical. Fig. 11, *A* and *B*, shows that over the range of ammonium sulfate concentrations investigated the aggregates correspond to a gel. A liquid-liquid phase separation may be detected in a small window at lower salt concentrations and higher protein concentrations. However, its existence is possible only if the gelation line intersects the binodal at a volume fraction above the critical point.

The effect of the range of the interaction potential on the gelation line was investigated theoretically by Noro et al. (85) and by Foffi et al. (52,86). They found that for a very short-ranged attraction the gelation line can intersect the binodal at a volume fraction below the critical point, in which case a liquid-liquid phase separation is impossible and a gas-liquid phase separation systematically leads to the formation of a gel. However, parameters such as protein anisotropy can come into play (87–89), and as theoretical phase diagrams are based on highly idealized representations of the interaction potential between proteins, only qualitative comparisons are meaningful. It is not possible to conclude in the absence of experimental evidence whether or not a liquid-liquid phase separation should occur for ovalbumin and lysozyme in ammonium sulfate. Ideally, predictive approaches should be based on realistic pair potentials, including structural information, but only a few advanced calculations of protein phase behavior have been attempted to represent protein interactions more realistically (87–89).

Most of the phase diagram also corresponds to concentrated protein solutions (Fig. 11), whereas practical applications such as protein crystallization are generally performed at very low volume fractions. In typical crystallization experiments the starting protein concentration is 10–40 mg/mL (17), which corresponds to a volume fraction of ~0.007–

0.03 (Fig. 11 *D*). Fig. 11, *A* and *B*, shows that the aggregates obtained for ovalbumin and lysozyme in ammonium sulfate starting from a solution at such a concentration correspond to a gel, and the same applies to lysozyme in sodium chloride. In this context, the precipitates observed during crystallization trials using salt precipitants likely correspond to gel phases.

Comparison between b_2 and the aggregation line

The comparison between experimental and theoretical phase diagrams given here is based on the correspondence between decreasing T^* and increasing salt concentration. This is based implicitly on the increasingly attractive trend in protein interactions with increasing salt concentration during protein salting-out, which is the only aspect of the phase behavior investigated here. The osmotic second virial coefficient provides an experimental measure of protein interactions that can be correlated with the resulting phase behavior. The second osmotic virial coefficient is expressed here as the dimensionless quantity $b_2 = B_{22}/B_{22}^{HS}$, where B_{22} is the dimensional osmotic second virial coefficient and the denominator is the excluded volume (hard sphere) contribution to protein-protein interactions. By definition, positive b_2 values generally correspond to repulsive interactions whereas negative values correspond to attractive interactions.

Among the six proteins investigated here, b_2 has been reported at pH 7 for ovalbumin, ribonuclease A, lysozyme in ammonium sulfate (76,90), and lysozyme in sodium chloride (91). Fig. 12 shows the comparison between the literature b_2 values for these systems and the aggregation lines obtained under the same solution conditions. The lysozyme crystal solubility in sodium chloride at pH 7 is also compared to the corresponding b_2 values in Fig. 12 *D*.

The comparison shows that for these three proteins, aggregation occurs in the general vicinity of the b_2 drop toward negative values. This correlation, which is in the spirit of the crystallization slot defined by George and Wilson (43,44), is not surprising as it indicates that proteins precipitate when interactions become more attractive. However, for some proteins the b_2 drop is followed immediately by precipitation, whereas for others it happens at significantly higher salt concentrations, showing that each protein has distinctive precipitation behavior.

The phase behavior depends in a complex fashion on the heterogeneity and anisotropy of protein interactions. Because, b_2 is only a highly averaged measure of protein interactions that provides an incomplete picture of protein interactions, it is an imperfect predictor of protein phase behavior. There is nevertheless sufficient agreement to identify an equivalence of the information obtained from b_2 and from the aggregation line. Therefore, both can be used to indicate the region favorable to protein crystallization (16,17,43,44).

Based on the theoretical phase diagram (Fig. 1), the area below the solubility line corresponds to the metastable region in which proteins may crystallize if nucleation occurs (46, 48,50,51). The gas-liquid phase separation that corresponds to the aggregation line is consequently one of the best indicators of the location of the metastable region. Aggregation occurs readily, and if the focus is to find favorable conditions for crystal growth, even the most efficient methods to measure b_2 cannot compete in time and protein consumption with very simple screening techniques. This justifies the common practice in crystallization screens of adjusting the precipitant concentration around solution conditions leading to aggregate formation (16,17). Nevertheless, b_2 has the advantage of providing information on repulsive interactions and the extent of the region over which protein crystallization is possible.

The relation between b_2 and phase behavior is a direct consequence of the central role played by the PMF. Experimentally, the connection between b_2 and protein solubility (92–94) has been an important recent focus of research. However, because protein crystal solubility is a function of the nature of the solid phase, its relation to b_2 is even more complex than the correlation between b_2 and the aggregation line. The phase behavior of proteins is often associated with crystal solubility, but the results here show that only the aggregation line allows systematic investigation of protein phase behavior. In contrast to crystalline phases, which may not exist under certain solution conditions and for which nucleation is usually highly variable, nonequilibrium phases typically form readily, as evidenced by the results for the different proteins investigated here.

Effects of temperature on protein phase behavior

The results presented in the previous three sections show relatively good qualitative agreement with the theoretical predictions in Fig. 1. All of these experiments were performed at 23°C and increasing salt concentration, i.e., T^* was varied by manipulating ε. This is a natural choice as most protein crystallization experiments are conducted isothermally by varying the precipitant concentration. However, the effect of temperature is also investigated here by replicating the phase behavior experiments at 4°C and 37°C.

Fig. 13 shows the temperature dependence of the phase behavior of ovalbumin, ribonuclease A, STI, β-lactoglobulin A and B, and lysozyme in ammonium sulfate, and Fig. 14 shows corresponding data for lysozyme in sodium chloride. The seven systems investigated display four different types of behavior. The aggregate solubility of lysozyme increased with increasing temperature in both ammonium sulfate and sodium chloride, whereas ovalbumin and β-lactoglobulin A and B exhibited the opposite behavior, i.e., they displayed retrograde aggregate solubility with increasing temperature. A third type of behavior was observed for ribonuclease A in which aggregate solubility showed a minimum around room temperature. The last type of behavior is that of STI, for which the aggregation line did not depend on temperature.

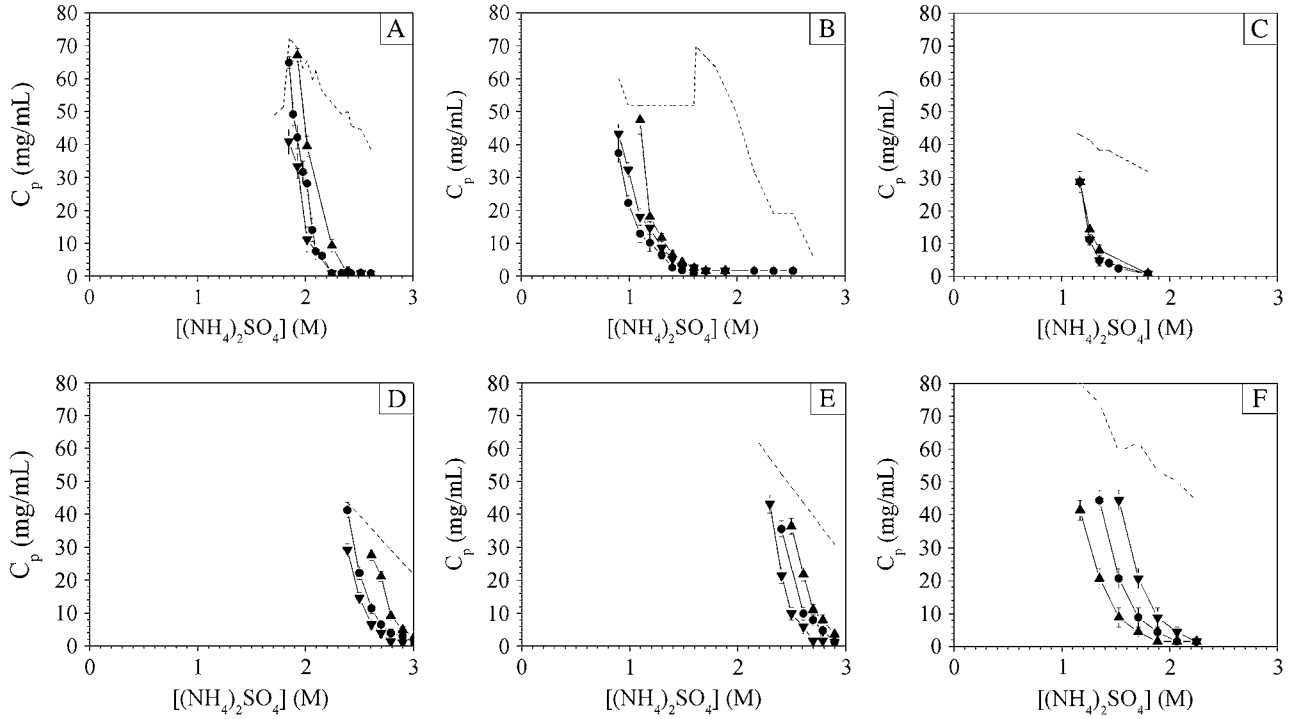

FIGURE 13 Effect of temperature on aggregation line for (*A*) ovalbumin, (*B*) ribonuclease A, (*C*) STI, (*D*) β-lactoglobulin A, (*E*) β-lactoglobulin B, and (*F*) lysozyme as a function of $(NH_4)_2SO_4$ concentration at pH 7. (▲) 4°C, (●) 23°C, (▼) 37°C. The buffer concentration was 100 mM sodium phosphate for STI and ribonuclease A, and 5 mM sodium phosphate for ovalbumin, β-lactoglobulin A and B, and lysozyme. The dotted line delimits the domain investigated experimentally.

Lysozyme also exhibited a much stronger temperature dependence in sodium chloride than it did in ammonium sulfate (Figs. 13 and 14). This observation is consistent with results reported in the literature (23,30,32). The magnitude of the temperature dependence in sodium chloride facilitates the investigation of lysozyme, and this probably contributed to the predilection for studying this particular system as a function of temperature. γ-Crystallins (18–20) and BPTI (37,38) show the same temperature dependence, but comparison with these results suggests that this behavior is not as common as it may seem.

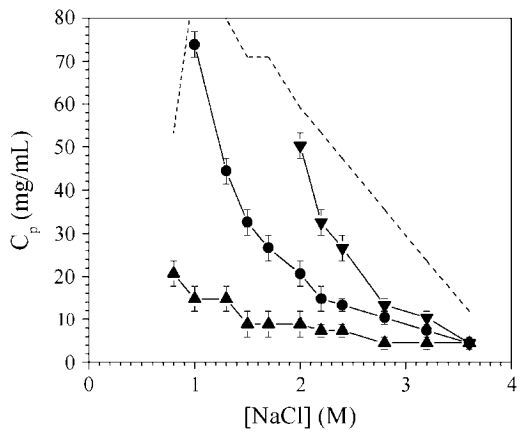

FIGURE 14 Effect of temperature on aggregation line for lysozyme as a function of NaCl concentration in 5 mM sodium phosphate, pH 7. (▲) 4°C, (●) 23°C, (▼) 37°C. The dotted line delimits the domain investigated experimentally.

Overall, the theoretical phase diagram obtained from a short-range Yukawa potential captures some important qualitative aspects of the experimental phase diagrams of proteins. However, the experimental trends as a function of temperature for most proteins investigated here are inconsistent with the theoretical prediction that the protein aggregate solubility should increase with increasing temperature (Fig. 1). The trends for ovalbumin, ribonuclease A, and β-lactoglobulin A and B are in clear disagreement with the theoretical phase diagram in Fig. 1. The proteins investigated are not exceptions, as retrograde solubility dependence at high salt concentrations has long been recognized for crystal and aggregate solubilities (4,10,95) and for b_2 (96). Protein salting-in was said by Cohn and Edsall (2) to follow a normal solubility dependence, whereas protein salting-out was then believed to follow a retrograde solubility trend. In this context, the temperature dependence of lysozyme in sodium chloride and ammonium sulfate would have been regarded as unusual.

From a theoretical point of view, retrograde solubility dependence on temperature suggests that a short-range attractive Yukawa potential does not capture all the features

important to protein interactions. To reproduce the trend as a function of increasing temperature, it would be necessary to introduce temperature dependence in the PMF. One possible interpretation of the entropic nature of such a contribution would be to attribute this effect to protein hydration forces, i.e., removal of water between protein interfaces on contact formation.

CONCLUSIONS

The theoretical predictions of protein phase behavior based on a simple colloidal model are in good qualitative agreement with the experimental phase behavior studied here for seven proteins at 23°C. In the theoretical framework offered by colloidal physics, protein crystals correspond to the thermodynamic equilibrium, whereas the liquid-liquid phase separation observed for proteins is viewed as a metastable state that occurs in the absence of crystal nucleation. The formation of gels and reversible aggregates is interpreted as two manifestations of the same phenomenon, corresponding to a frustrated liquid-liquid phase separation that can be explained theoretically by the predictions of MCT. The existence, for some proteins, of a second aggregation line is interpreted theoretically as the spinodal line that delimits the region beyond which aggregation occurs by spinodal decomposition instead of nucleation and for which the kinetics of aggregation differ. The results show that only a weak correlation exists between b_2 and the aggregation line and thus between b_2 and protein crystal solubility. Despite their success in explaining the general features of phase behavior, theoretical predictions fail to reproduce the trends as a function of temperature for most proteins. The temperature dependence suggests the importance of entropic effects, probably due to hydration forces that are not included in simple models such as the Yukawa potential. However, the main conclusion is the primary importance in real systems of nonequilibrium states such as liquid-liquid phase separation, gels, and aggregates that correspond to the most common manifestations of protein phase behavior.

We are grateful for support from the National Science Foundation (grant No. BES-0519191).

REFERENCES

1. Tanford, C., and J. A. Reynolds. 2001. Nature's Robots: A History of Proteins. Oxford University Press, New York.
2. Cohn, E. J., and J. T. Edsall. 1943. Proteins, Amino Acids and Peptides as Ions and Dipolar Ions. Reinhold Publishing, New York.
3. Arakawa, T., and S. N. Timasheff. 1985. Theory of protein solubility. *Methods Enzymol.* 114:49–77.
4. Green, A. A. 1931. Studies in the physical chemistry of the proteins: VIII. The solubility of hemoglobin in concentrated salt solutions. A study of the salting out of proteins. *J. Biol. Chem.* 93:495–516.
5. Green, A. A. 1931. Studies in the physical chemistry of the proteins: IX. The effect of electrolytes on the solubility of hemoglobin in solutions of varying hydrogen ion activity with a note on the comparable behavior of casein. *J. Biol. Chem.* 93:517–542.
6. Kunz, W., J. Henle, and B. W. Ninham. 2004. Zur Lehre von der Wirkung de Salze (about the science of the effect of salts): Franz Hofmeister's historical papers. *Curr. Opin. Colloid Interface Sci.* 9: 19–37.
7. Hofmeister, F. 1888. Zur Lehre von der Wirkung der Salze. *Arch. Exp. Pathol. Pharmakol.* 24:247–260.
8. Butler, J. A. V. 1940. The use of solubility as a criterion of purity of proteins. *J. Gen. Physiol.* 24:189–202.
9. Sörensen, S. P. L. 1925. The solubility of proteins. *J. Am. Chem. Soc.* 47:457–469.
10. Bunn, C. W., P. C. Moews, and M. E. Baumber. 1971. The crystallography of calf rennin (chymosin). *Proc. R. Soc. Lond. B. Biol. Sci.* 178:245–258.
11. Feher, G., and Z. Kam. 1985. Nucleation and growth of protein crystals: general principles and assays. *Methods Enzymol.* 114:77–112.
12. Shih, Y.-C., J. M. Prausnitz, and H. W. Blanch. 1992. Some characteristics of protein precipitation by salts. *Biotechnol. Bioeng.* 40:1155–1164.
13. Rousseau, F., J. Schymkowitz, and L. Serrano. 2006. Protein aggregation and amyloidosis: confusion of the kinds? *Curr. Opin. Struct. Biol.* 16:118–126.
14. Dobson, C. M. 2003. Protein folding and misfolding. *Nature.* 426: 884–890.
15. Krebs, M. R. H., G. L. Devlin, and A. M. Donald. 2007. Protein particulates: another generic form of protein aggregation? *Biophys. J.* 92:1336–1342.
16. Gilliland, G. L., and D. R. Davies. 1984. Protein crystallization: the growth of large-scale single crystals. *Methods Enzymol.* 104:370–381.
17. McPherson, A. 1999. Crystallization of Biological Macromolecules. Cold Spring Harbor Laboratory Press, Cold Spring Harbor, NY.
18. Thomson, J. A., P. Schurtenberger, G. M. Thurston, and G. B. Benedek. 1987. Binary liquid phase separation and critical phenomena in protein/water solution. *Proc. Natl. Acad. Sci. USA.* 84:7079–7083.
19. Broide, M. L., C. R. Berland, J. Pande, O. Ogun, and G. B. Benedek. 1991. Binary-liquid phase-separation of lens protein solutions. *Proc. Natl. Acad. Sci. USA.* 88:5660–5664.
20. Berland, C. R., G. M. Thurston, M. Kondo, M. L. Broide, J. Pande, O. Ogun, and G. B. Benedek. 1992. Solid-liquid phase boundaries of lens protein solution. *Proc. Natl. Acad. Sci. USA.* 89:1214–1218.
21. Tanaka, T., C. Ishimoto, and L. T. Chylack. 1977. Phase separation of a protein-water mixture in cold cataract in the young rat lens. *Science.* 197:1010–1012.
22. Ishimoto, C., and T. Tanaka. 1977. Critical behavior of a binary mixture of protein and salt water. *Phys. Rev. Lett.* 39:474–477.
23. Taratuta, V. G., A. Holschbach, G. M. Thurston, D. Blankschtein, and G. B. Benedek. 1990. Liquid-liquid phase separation of aqueous lysozyme solutions: effects of pH and salt identity. *J. Phys. Chem.* 94:2140–2144.
24. Phillies, G. D. J. 1985. Comment on ''Critical behavior of a binary mixture of protein and salt water''. *Phys. Rev. Lett.* 55:1341.
25. Muschol, M., and F. Rosenberger. 1997. Liquid-liquid phase separation in supersaturated lysozyme solutions and associated precipitate formation/crystallization. *J. Chem. Phys.* 107:1953–1962.
26. Schurtenberger, P., R. A. Chamberlin, G. M. Thurston, J. A. Thomson, and G. B. Benedek. 1989. Observation of critical phenomena in a protein-water solution. *Phys. Rev. Lett.* 63:2064–2067.
27. Manno, M., C. Xiao, D. Bulone, V. Martorana, and P. L. San Biagio. 2003. Thermodynamic instability in supersaturated lysozyme solutions: effect of salt and role of concentration fluctuations. *Phys. Rev. E.* 68:11904.
28. Yeomans, J. M. 1992. Statistical Mechanics of Phase Transitions. Oxford University Press, New York.
29. Broide, M. L., T. M. Tominc, and M. D. Saxowsky. 1996. Using phase transitions to investigate the effect of salts on protein interactions. *Phys. Rev. E.* 53:6325–6335.

30. Grigsby, J. J., H. W. Blanch, and J. M. Prausnitz. 2001. Cloud-point temperature for lysozyme in electrolyte solutions: effect of salt type, salt concentration and pH. *Biophys. Chem.* 91:231–243.

31. Tanaka, S., M. Ataka, and K. Ito. 2002. Pattern formation and coarsening during metastable phase separation in lysozyme solutions. *Phys. Rev. E.* 65:51804.

32. Tanaka, S., M. Yamamoto, K. Ito, and R. Hayakawa. 1997. Relation between the phase separation and the crystallization in protein solutions. *Phys. Rev. E.* 56:R67–R69.

33. Tanaka, H., and Y. Nishikawa. 2005. Viscoelastic phase separation of protein solutions. *Phys. Rev. E.* 95:078103.

34. Vekilov, P. G. 2005. Two-step mechanism for the nucleation of crystals from solution. *J. Cryst. Growth.* 275:65–76.

35. Galkin, O., and P. G. Vekilov. 2000. Control of protein crystal nucleation around the metastable liquid-liquid phase boundary. *Proc. Natl. Acad. Sci. USA.* 97:6277–6281.

36. Filobelo, L. F., O. Galkin, and P. G. Vekilov. 2005. Spinodal for the solution-to-crystal phase transformation. *J. Chem. Phys.* 123:14904–14911.

37. Grouazel, S., J. Perez, J.-P. Astier, F. Bonneté, and S. Veesler. 2002. BPTI liquid-liquid phase separation monitored by light and small angle x-ray scattering. *Acta Crystallogr. D Biol. Crystallogr.* 58:1560–1563.

38. Grouzael, S., F. Bonneté, J. P. Astier, N. Ferté, J. Perez, and S. Veesler. 2006. Exploring bovine pancreatic trypsin inhibitor phase transitions. *J. Phys. Chem. B.* 110:19664–19670.

39. Kulkarni, A. M., N. M. Dixit, and C. F. Zukoski. 2003. Ergodic and non-ergodic phase transitions in globular protein suspensions. *Faraday Discuss. Chem. Soc.* 123:37–50.

40. Sedgwick, H., K. Kroy, A. Salonen, M. B. Robertson, S. U. Egelhaaf, and W. C. K. Poon. 2005. Non-equilibrium behavior of sticky colloidal particles: bead, cluster and gels. *Eur. Phys. J. E.* 16:77–80.

41. Cheng, Y.-C., R. F. Lobo, S. I. Sandler, and A. M. Lenhoff. 2006. Kinetics and equilibria of lysozyme precipitation and crystallization in concentrated ammonium sulfate solutions. *Biotechnol. Bioeng.* 94:177–188.

42. Curtis, R. A., J. Newman, H. W. Blanch, and J. M. Prausnitz. 2001. McMillan-Mayer solution thermodynamics for a protein in a mixed solvent. *Fluid Phase Equil.* 192:131–153.

43. George, A., and W. W. Wilson. 1994. Predicting protein crystallization from a dilute-solution property. *Acta Crystallogr. D Biol. Crystallogr.* 50:361–365.

44. George, A., Y. Chiang, B. Guo, A. Arabshahi, Z. Cai, and W. W. Wilson. 1997. Second virial coefficient as predictor in protein crystal growth. *Methods Enzymol.* 276:100–110.

45. Rosenbaum, D., P. C. Zamora, and C. F. Zukoski. 1996. Phase behavior of small attractive colloidal particles. *Phys. Rev. Lett.* 76:150–153.

46. Rosenbaum, D. F., and C. F. Zukoski. 1996. Protein interactions and crystallization. *J. Cryst. Growth.* 169:752–758.

47. Poon, W. C. K. 1997. Crystallization of globular proteins. *Phys. Rev. E.* 55:3762–3764.

48. Piazza, R. 1999. Interactions in protein solutions near crystallization: a colloid physics approach. *J. Cryst. Growth.* 196:415–423.

49. Vliegenthart, G. A., and H. N. W. Lekkerkerker. 2000. Predicting the gas-liquid critical point from the second virial coefficient. *J. Chem. Phys.* 112:5364–5369.

50. Haas, C., and J. Drenth. 1998. The protein-water phase diagram and the growth of protein crystals from aqueous solution. *J. Phys. Chem. B.* 102:4226–4232.

51. Haas, C., and J. Drenth. 1999. Understanding protein crystallization on the basis of the phase diagram. *J. Cryst. Growth.* 196:388–394.

52. Foffi, G., G. D. McCullagh, A. Lawlor, E. Zaccarelli, K. A. Dawson, F. Sciortino, P. Tartaglia, D. Pini, and G. Stell. 2002. Phase equilibria and glass transition in colloidal systems with short-ranged attractive interactions: application to protein crystallization. *Phys. Rev. E.* 65:31407.

53. Asthagiri, D., B. L. Neal, and A. M. Lenhoff. 1999. Calculation of short-range interactions between proteins. *Biophys. Chem.* 78:219–231.

54. Hloucha, M., J. F. M. Lodge, A. M. Lenhoff, and S. I. Sandler. 2001. A patch-antipatch representation of specific protein interactions. *J. Cryst. Growth.* 232:195–203.

55. Tavares, F. W., and J. M. Prausnitz. 2004. Analytic calculation of phase diagrams for solutions containing colloids or globular proteins. *Colloid Polym. Sci.* 282:620–632.

56. Hagen, M. H. J., and D. Frenkel. 1994. Determination of phase diagrams for the hard-core attractive Yukawa system. *J. Chem. Phys.* 101:4093–4097.

57. Dawson, K. A., G. Foffi, M. Fuchs, W. Götze, F. Sciortino, M. Sperl, P. Tartaglia, T. Voigtmann, and E. Zaccarelli. 2000. Higher-order glass-transition singularities in colloidal systems with attractive interactions. *Phys. Rev. E.* 63:11401–11418.

58. Pham, K. N., A. M. Puertas, J. Bergenholtz, S. U. Egelhaaf, A. Moussaid, P. N. Pusey, A. B. Schofield, M. E. Cates, M. Fuchs, and W. C. K. Poon. 2002. Multiple glassy states in a simple model system. *Science.* 296:104–106.

59. Dawson, K. A. 2002. The glass paradigm for colloidal glasses, gels, and other arrested states driven by attractive interactions. *Curr. Opin. Colloid Interface Sci.* 7:218–227.

60. Fabbian, L., W. Götze, F. Sciortino, P. Tartaglia, and F. Thiery. 1999. Ideal glass-glass transitions and logarithmic decay of correlations in a simple system. *Phys. Rev. E.* 59:R1347–R1350.

61. Bergenholtz, J., and M. Fuchs. 1999. Non-ergodicity transitions in colloidal suspensions with attractive interactions. *Phys. Rev. E.* 59: 5706–5715.

62. Zaccarelli, E., F. Sciortino, P. Tartaglia, G. Foffi, G. D. McCullagh, A. Lawlor, and K. A. Dawson. 2002. Competition between crystallization and glassification for particles with short-ranged attraction. Possible applications to protein crystallization. *Physica A.* 314:539–547.

63. Gottschalk, A., and B. Graham. 1966. The basic structure of glycoproteins. *In* The Proteins. H. Neurath, editor. Academic Press, New York. 95–151.

64. Tanford, C., and J. D. Hauenstein. 1956. Hydrogen ion equilibria of ribonuclease. *J. Am. Chem. Soc.* 78:5287–5291.

65. Roychaudhuri, R., G. Sarath, M. Zeece, and J. Markwell. 2003. Reversible denaturation of the soybean Kunitz trypsin inhibitor. *Arch. Biochem. Biophys.* 412:20–26.

66. Kunitz, M. 1945. Crystalline soybean trypsin inhibitor. II. General properties. *J. Gen. Physiol.* 29:149–154.

67. Treece, J. M., R. S. Sheinson, and T. L. McMeekin. 1964. The solubilities of β-lactoglobulins A, B and AB. *Arch. Biochem. Biophys.* 108:99–108.

68. Brownlow, S., J. H. M. Cabral, R. Cooper, D. R. Flower, S. J. Yewdall, I. Polikarpov, A. C. T. North, and L. Sawyer. 1997. Bovine β-lactoglobulin at 1.8 Å resolution. Still an enigmatic lipocalin. *Structure.* 5:481–495.

69. Tanford, C., and M. L. Wagner. 1954. Hydrogen ion equilibria of lysozyme. *J. Am. Chem. Soc.* 76:3331–3336.

70. Gilliland, G. L. 1988. A biological macromolecule crystallization database: a basis for a crystallization strategy. *J. Cryst. Growth.* 90:51–59.

71. Kunitz, M. 1945. Crystallization of a trypsin inhibitor from soybean. *Science.* 101:668–669.

72. Palmer, A. H. 1934. The preparation of a crystalline globulin from the albumin fraction of cow's milk. *J. Biol. Chem.* 104:359–372.

73. Judge, R. A., M. R. Johns, and E. T. White. 1995. Protein purification by bulk crystallization: the recovery of ovalbumin. *Biotechnol. Bioeng.* 48:316–323.

74. Sörensen, S. P. L., and M. Höyrup. 1915. On the preparation of egg-albumin solutions of well-defined composition, and on the analytical methods used. *C. R. Trav. Lab. Carlsberg.* 12:12–67.

75. Sober, H. A., editor. 1970. Handbook of Biochemistry. Selected Data for Molecular Biology. The Chemical Rubber Company, Cleveland, OH.

76. Dumetz, A. C., A. M. Snellinger-O'Brien, E. W. Kaler, and A. M. Lenhoff. 2007. Patterns of protein-protein interactions in salt solutions and implications for protein crystallization. *Protein Sci.* 16:1867–1877.

77. Petsev, D. N., X. Wu, O. Galkin, and P. G. Vekilov. 2003. Thermodynamic functions of concentrated protein solutions from phase equilibria. *J. Phys. Chem. B.* 107:3921–3926.

78. Verduin, H., and J. K. G. Dhont. 1995. Phase diagram of a model adhesive hard-sphere dispersion. *J. Colloid Interface Sci.* 172:425–437.

79. Bhat, S., R. Tuinier, and P. Schurtenberger. 2006. Spinodal decomposition in a food colloid-biopolymer mixture: evidence for a linear regime. *J. Phys. Condens. Matter.* 18:L339–L346.

80. Verhaegh, N. A. M., D. Asnaghi, H. N. W. Lekkerkerker, M. Giglio, and L. Cipelletti. 1997. Transient gelation by spinodal decomposition in colloid-polymer mixtures. *Physica A.* 242:107–118.

81. Koenderink, G. H., D. G. A. L. Aarts, V. W. A. de Villeneuve, A. P. Philipse, R. Tuinier, and H. N. W. Lekkerkerker. 2003. Morphology and kinetics of phase separating transparent xanthan-colloid mixtures. *Macromolecules.* 4:129–136.

82. Verhaegh, N. A. M., J. S. van Duijneveldt, J. K. G. Dhont, and H. N. W. Lekkerkerker. 1996. Fluid-fluid phase separation in colloid-polymer mixtures studied with small angle light scattering and light microscopy. *Physica A.* 230:409–436.

83. Stradner, A., H. Sedgwick, F. Cardinaux, W. C. K. Poon, S. U. Dgelhaaf, and P. Schurtenberger. 2004. Equilibrium cluster formation in concentrated protein solutions and colloids. *Nature.* 432:492–495.

84. Stradner, A., F. Cardinaux, and P. Schurtenberger. 2006. A small-angle scattering study on equilibrium clusters in lysozyme solutions. *J. Phys. Chem. B.* 110:21222–21231.

85. Noro, M. G., N. Kern, and D. Frenkel. 1999. The role of long-range forces in the phase behavior of colloids and proteins. *Europhys. Lett.* 48:332–338.

86. Foffi, G., C. De Michele, F. Sciortino, and P. Tartaglia. 2005. Scaling of dynamics with the range of interaction in short-range attractive colloids. *Phys. Rev. Lett.* 94:078301.

87. Lomakin, A., N. Asherie, and G. B. Benedek. 1999. Aeolotopic interactions of globular proteins. *Proc. Natl. Acad. Sci. USA.* 96:9465–9468.

88. Kern, N., and D. Frenkel. 2003. Fluid-fluid coexistence in colloidal systems with short-ranged strongly directional attraction. *J. Chem. Phys.* 118:9882–9889.

89. Chang, J., A. M. Lenhoff, and S. I. Sandler. 2004. Determination of fluid-solid transitions in model protein solutions using the histogram reweighting method and expanded ensemble simulations. *J. Chem. Phys.* 120:3003–3014.

90. Curtis, R. A., J. Ulrich, A. Montaser, J. M. Prausnitz, and H. W. Blanch. 2002. Protein-protein interactions in concentrated electrolyte solutions. Hofmeister-series effects. *Biotechnol. Bioeng.* 79:367–380.

91. Tessier, P. M., A. M. Lenhoff, and S. I. Sandler. 2002. Rapid measurement of protein osmotic second virial coefficients by self-interaction chromatography. *Biophys. J.* 82:1620–1631.

92. Haas, C., J. Drenth, and W. W. Wilson. 1999. Relation between the solubility of proteins in aqueous solutions and the second virial coefficient of the solution. *J. Phys. Chem. B.* 103:2808–2811.

93. Guo, B., S. Kao, H. McDonald, A. Asanov, L. L. Combs, and W. W. Wilson. 1999. Correlation of second virial coefficients and solubilities useful in protein crystal growth. *J. Cryst. Growth.* 196:424–433.

94. Demoruelle, K., B. Guo, S. Kao, H. M. Mcdonald, D. B. Nikic, S. C. Holman, and W. W. Wilson. 2002. Correlation between the osmotic second virial coefficient and solubility for equine serum albumin and ovalbumin. *Acta Crystallogr. D Biol. Crystallogr.* 58:1544–1548.

95. Cohn, E. J. 1925. The physical chemistry of the proteins. *Physiol. Rev.* 5:349–437.

96. Wilson, W. W. 2003. Light scattering as a diagnostic for protein crystal growth—a practical approach. *J. Struct. Biol.* 142:56–65.